

High temperature annealing of rare-earth implanted GaN

K. Lorenz, U. Wahl, E. Alves, S. Dalmaso¹, R.W. Martin¹, K.P. O'Donnell¹, T. Wojtowicz², P. Ruterana², S. Ruffenach³, O. Briot³

Objectives

In the frame of the European Research Training Network project RENiBEL (Rare Earth doped Nitrides for high Brightness Electroluminescent devices) we study rare earth (RE) doping by ion implantation into GaN films. Ion implantation is a technique to realize the rare earth doping of planar substrates with the facility of lateral patterning. However, the radiation damage produced by implantation of heavy ions proves difficult to be removed in this material. In particular the regrowth of amorphous layers is still an open problem. To integrate ion implantation into device production technology it is essential to study and understand the damage build-up and the amorphisation processes during implantation.

Results

In this year's work we focussed on the influence of a thin AlN capping layer on the damage build-up in rare earth implanted GaN. The 10 nm thin AlN layer was deposited by MOCVD during the growth of the GaN material prior to the implantation.

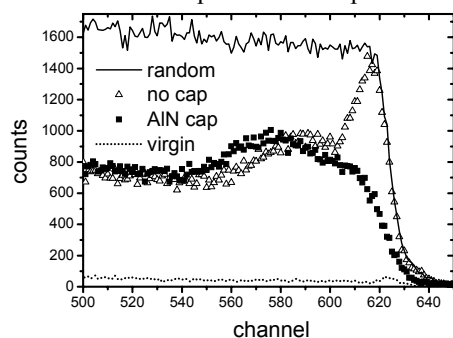


Fig. 1. RBS/C random and $\langle 0001 \rangle$ -aligned spectra of GaN implanted with 2×10^{15} Eu/cm².

Figure 1 shows the typical damage behaviour of uncapped GaN and the influence of the AlN cap for implantation of 300 keV Eu ions with a fluence of 2×10^{15} at/cm².

For implantation in uncapped material two damage regions can be distinguished in the aligned RBS/C spectra: one at the surface and another one extending deeper into the bulk of the crystal coinciding with the end of range of the implanted ions. The surface peak reaches the random spectrum indicating an amorphisation of the surface layer. The thickness of this amorphous layer increases with the implantation fluence as it was confirmed by TEM measurements, and during post-implant annealing it often leads to an increased dissociation of the sample at temperatures around 1000 °C. The amorphisation can be inhibited by implanting through the AlN capping layer, as it can

be concluded from the RBS/C spectra in figure 1. For the capped sample no surface peak is visible.

A second purpose of the capping layer is to protect the surface from out-diffusion of nitrogen during high-temperature annealing. After annealing the samples up to 1300 °C no signs of dissociation of the crystal or RE diffusion were observed for samples implanted with fluences lower than 1×10^{15} at/cm². Optical activation of the rare earth ions with the typical intra-ionic emission lines was achieved after high temperature annealing. Figure 2 shows cathodoluminescence (CL) spectra taken at room temperature of AlN-capped GaN implanted with 1×10^{15} at/cm² Eu. Remarkably, the emission intensity increases by one order of magnitude within the studied annealing range between 1100 and 1300 °C.

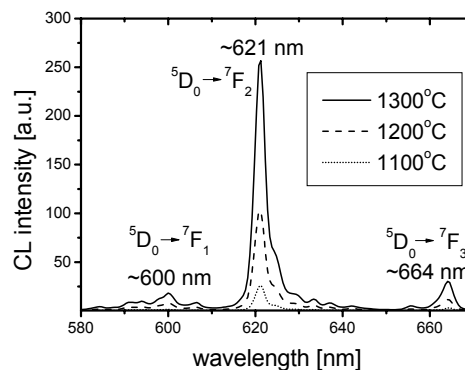


Fig. 2. CL spectra of AlN-capped GaN implanted with Eu and annealed between 1100 and 1300 °C.

Published, accepted or in press work

1. K. Lorenz, U. Wahl, E. Alves, T. Wojtowicz, P. Ruterana, S. Ruffenach, O. Briot, Amorphisation of GaN during processing with rare earth ion beams, *Superlattices and Microstructures* **36** (2004) 737.
2. A. Colder, P. Marie, T. Wojtowicz, P. Ruterana, S. Eimer, L. Méchin, K. Lorenz, U. Wahl, E. Alves, V. Matias, M. Mamor, B. Pipeleers, A. Vantomme, Characterisation of defects in rare earth implanted GaN by Deep Level Transient Spectroscopy, *Superlattices and Microstructures* **36** (2004) 713.
3. K. Lorenz, U. Wahl, E. Alves, S. Dalmaso, R. W. Martin, K. P. O'Donnell, S. Ruffenach, O. Briot, High temperature annealing and optical activation of Eu implanted GaN, *Appl. Phys. Lett.* **85** (2004) 2712.
4. K. Lorenz, *et al.*, Optical doping of AlN by rare earth implantation, *NIM B* (accepted)

¹Dep. of Physics, Strathclyde University, Scotland

²CIRIL-ENSICAEN- Caen, France

³GES, Montpellier, France

Structural characterization of Ge/Si quantum dots

A. Fonseca, E. Alves, N. Franco, J. P. Leitão¹, N. A. Sobolev¹

Objectives

In present work we study Ge islands growth in Si substrate. Two types of samples are under study: the first one, Ge dots are grown by Stranski-Krastanov mechanism, that result the appearance the Ge islands on the top a quantum well (wetting layer – WL), this method permit the appearance of islands highly ordered with lateral density up to $1 \times 10^{11} \text{ cm}^{-2}$; the second type of dots are growth in an ultra thin layer of SiO₂, with this new method one can obtain Ge islands with higher density and small size. These Ge/Si dots are useful for electronic devices, integrated circuits, lasers and for several applications in microelectronic devices.

Results

In this year's work we focussed our studies in the structural characterization through X-ray diffraction, and Rutherford Backscattering Spectroscopy (RBS), of Si/Ge samples with Ge islands. Some work was done on optical characterization with photoluminescence.

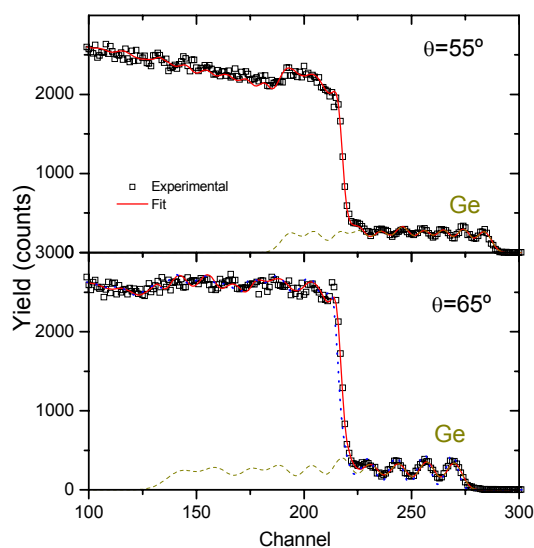


Fig. 1. RBS spectra collected at 55° and 65° of the sample with 10 period Ge/Si multilayers.

The first set of samples (5 and 10 period Ge/Si multilayers) shows the existence of Ge dots, and that periodicity of sample is an important factor to growth coherent quantum dots (sample with 10 periods shows coherent QD, and with 5 dots were uncorrelated). Samples grown on a SiO₂ layer and with a layer of 3, 6 or 9 Å Ge, are more difficult to characterize though X-ray diffraction due to their lower percentage of Ge, and due to do not have periodicity.

To characterize these samples we use RBS at grazing angles of incidence and some channelling studies were done to get some information on the strain state of the layers. Figure 1 shows typical RSB spectra for tilted

angles for sample with 10 periods. We observe that Ge layer have some thicker regions that could correspond to the quantum dots (this can be compared with TEM results).

Figure 2 shows the angular scan of Ge/SiO₂ samples for <110> direction. With 3 Å of Ge we can see that the Ge atoms are perfectly aligned with Si atoms, the minimum yield is lower and almost equal to the Si, i. e, Ge atoms are substitutional to Si. For other samples, with higher thickness of Ge, is evident that Ge atoms are not aligned with Si and minimum yield is higher. There is an evidence for the destruction of the crystal

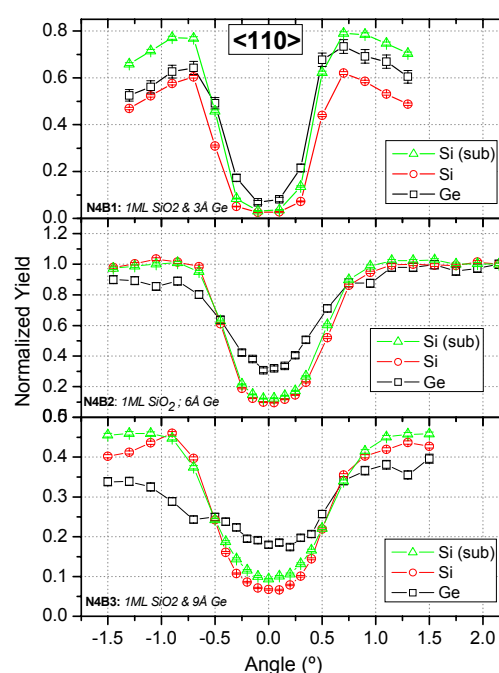


Fig. 2. Angular scan along <110> direction for Ge/SiO₂ samples (3, 6 and 9 Å of Ge). The broadening of the Ge curve and the high value of minimum yield suggest the formation of Ge islands, for sample with 9 Å of Ge.

lattice and the formation of Ge nanoprecipitates, the quantum dots.

Published, accepted or in press work

1. A. Fonseca, N. A. Sobolev, J. P. Leitão, M. C. Carmo, N. Franco, H. Presting, A. Sequeira, "Strutual characterization and luminescence of Ge/Si Quantum Dots", *Materials Science Forum* **455** (2004) 540;
2. A. Fonseca, N. Franco, E. Alves, N. P. Barradas, J. Leitão, N. A. Sobolev, D. Badonneau "High resolution backscattering studies of nanostructured magnetic and semiconducting materials", accepted for publication.

¹ Dep. Física, Universidade de Aveiro

Ion implantation doping of ZnO

E. Rita, E. Alves, U. Wahl, J.G. Correia, A.M.L. Lopes¹, T. Monteiro¹, J.C. Soares²,
The ISOLDE collaboration³

Objectives

This work explores the implantation of possible electrical, optical and ferromagnetic dopants into ZnO, a wide bandgap II-VI semiconductor of interest in optoelectronics and, more recently, for spintronics. The implantation and RBS/C studies were carried out at ITN. The EC studies were performed at CERN/ISOLDE and the optical measurements were done in collaboration with the University of Aveiro.

Results

1. Lattice site and stability of implanted Fe in ZnO

The Emission Channeling (EC) technique was applied to evaluate the lattice location of implanted ⁵⁹Fe (ferromagnetic dopant) in single-crystalline ZnO. Our results revealed that, following the 800°C vacuum annealing, 95(8)% of the Fe atoms are incorporated on ideal substitutional Zn sites with rms displacements as low as the thermal vibration amplitude of Zn atoms (0.06–0.09 Å).

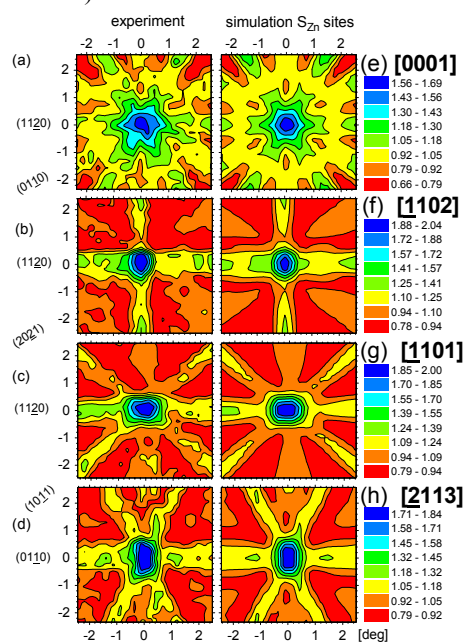


Fig.1. (a)-(d): β^- emission channeling patterns from ⁵⁹Fe-implanted ZnO after the 800°C vacuum annealing. (e)-(h): best fits of simulated channeling patterns to the experimental yields, corresponding to 95(8)% of ⁵⁹Fe on ideal S_{Zn} sites.

2. Rare-Earth - Tm implantations

ZnO single crystals were implanted with Tm ions at different fluences. The defect recovery, the Tm lattice location and its optical activation were investigated by means of the Rutherford Backscattering/Channeling Spectrometry (RBS/C) and Photoluminescence (PL) techniques. Damage recovery becomes significant for air annealing above 750°C and is almost complete at 1050°C. Implantation damage decreases for implantations at mild temperatures (450°C) and is also highly reduced for <0001> aligned implantations. Tm ions start to diffuse towards the surface above 900°C and about 80% of them have segregate to the surface after 90 min annealing at 1050°C. In the as-implanted state the optical activity of Tm is highly quenched by the implantation defects. While annealing at 800°C induces optical activation of these ions, diffusion to the surface at higher annealing temperatures destroys the luminescence. The highest intensity of Tm-related optical centres occurs for the 800°C air annealed samples implanted at 450°C with low fluence.

Published, accepted or in press work

1. E. Rita, U. Wahl, J.G. Correia, E. Alves, J.C. Soares, ISOLDE Collaboration, Lattice location and thermal stability of implanted Fe in ZnO, *Appl. Phys. Lett.* **85** (2004) 4899-4901.
2. U. Wahl, E. Rita, J.G. Correia, E. Alves, J.C. Soares, ISOLDE Collaboration, Lattice location and stability of implanted Cu in ZnO, *Physical Review B* **69** (2004) 012102.
3. M. Peres, J. Wang, M.J. Soares, A. Neves, T. Monteiro, E. Rita, U. Wahl, J.G. Correia, E. Alves, PL studies on ZnO single crystals implanted with thulium ions, *Superl. Microstr.* **36** (2004) 747-753.
4. E. Rita, J.G. Correia, U. Wah, E. Alves, A.M.L. Lopes, J.C. Soares, ISOLDE Collaboration, PAC studies of implanted ¹¹¹Ag in single-crystalline ZnO, Hyperfine Interactions, accepted for publication.
5. E. Rita, E. Alves, U. Wahl, J.G. Correia, T. Monteiro, M.J. Soares, A. Neves, M. Peres, Stability and luminescence studies of Tm and Er implanted ZnO single crystals, *Nucl. Instr. Meth. B*, accepted for publication.

¹ Dep. de Física, Universidade de Aveiro, 3810-193 Aveiro

² CFNUL, Av. Prof. Gama Pinto 2, 1699 Lisboa

³ CERN, CH-1211 Geneva 23, Switzerland

Emission channeling lattice location studies

U. Wahl, J.G. Correia, E. Rita, A.C. Marques, E. Alves, B. De Vries¹, S. Decoster¹,
A. Vantomme¹, J.C. Soares², and the ISOLDE collaboration³

Objectives

The aim of this work is to study the lattice location of impurities in technologically relevant semiconductors (e.g. Si, ZnO, GaN, diamond) and oxides (e.g. SrTiO₃, BaTiO₃) by means of emission channeling (EC) from radioactive isotopes. The experiments are carried out using the ITN/CFNUL infrastructure installed at CERN's ISOLDE facility. Additional EC results on ZnO are presented elsewhere in this report.

Results

1. Lattice location of rare earths in GaN

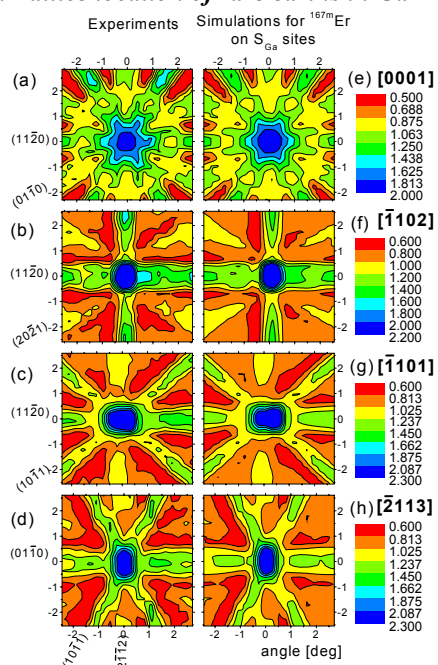


Fig. 1. Experimental EC patterns from ^{167m}Er in GaN (left) and simulations for Er on Ga sites (right).

The lattice location of implanted Er in GaN, GaN:O and GaN:C was investigated using conversion electrons emitted by the probe isotope ^{167m}Er [1]. The majority ($\approx 90\%$) of Er atoms are located on substitutional Ga sites in all 3 samples. Annealing up to 900°C did not change these fractions, although it reduced the Er root mean square (rms) displacements. The only visible effect of oxygen or carbon doping was a small increase in the rms displacements in comparison to the undoped sample.

2. New position-sensitive electron detectors for emission channeling

In collaboration with a CERN group specialized in position-sensitive detectors (PSDs), we have since several years been engaged in the development of advanced PSDs for electron detection. Currently, three setups (two from ITN/CFNUL, one from IKS Leuven) equipped with PSDs [4] are available for EC experiments at ISOLDE. Our aim for the future is to increase the number of isotopes which can be used by the EC technique. We are therefore currently working on PSDs equipped with a novel readout system that will allow measuring electrons with count rates in the 10 kHz regime and at energies down to 20 keV. Such detection systems will be required in future EC experiments, where it is intended to (a) work on-line with short-lived isotopes at very high count rates, or (b) detect very low energy conversion electrons below 40 keV. In 2004 prototypes of the new readout system have been successfully tested at CERN.

Published, accepted or in press work

1. B. De Vries, V. Matias, A. Vantomme, U. Wahl, E.M.C. Rita, E. Alves, A.M.L. Lopes, J.G. Correia, and the ISOLDE collaboration: "Influence of O and C co-implantation on the lattice site of Er in GaN", *Applied Physics Letters* **84** (2004) 4304-4306.
2. U. Wahl, J.G. Correia, E. Rita, E. Alves, J.C. Soares, B. De Vries, V. Matias, A. Vantomme, and the ISOLDE collaboration, "Recent emission channeling studies in wide band gap semiconductors", accepted by *Hyperfine Interactions*.
3. M. Dietrich, Ch. Buchal, J.G. Correia, M. Deicher, M. Schmid, M. Uhrmacher, U. Vetter, and U. Wahl: "Annealing of BaTiO₃ thin films after heavy ion implantation", *Nuclear Instruments and Methods in Physics Research B* **216** (2004) 110-115.
4. U. Wahl, J.G. Correia, A. Czermak, S.G. Jahn, P. Jalocha, J.G. Marques, A. Rudge, F. Schopper, A. Vantomme, P. Weilhammer, and the ISOLDE collaboration: "Position-sensitive Si pad detectors for electron emission channeling experiments", *Nuclear Instruments and Methods in Physics Research A* **524** (2004) 245-256.

¹ Instituut voor Kern- en Stralingsfysica, 3001 Leuven, Belgium

² CFNUL, Av. Prof. Gama Pinto 2, 1699 Lisboa

³ CERN, 1211 Geneva 23, Switzerland

Buried nanoprecipitates in MgO and TiO₂-rutile oxides

J.V. Pinto, C. Marques, N. Franco, E. Alves and R.C. da Silva

Objectives

The implantation of high fluences of transition metals has been used to promote the formation of metal clusters buried in insulator hosts, and induce optic, magnetic and electric modifications in such materials. These can be useful for switching, signaling, data transport, etc.

Our work concerns the ion beam synthesis of metallic and metal like nanoprecipitates buried in the crystalline oxides MgO, Al₂O₃, and TiO₂-rutile, and the changes in its structural, electric, magnetic and optical properties and stability.

Results

Ion beam synthesis of metallic nanoprecipitates in crystalline MgO and TiO₂-rutile

The work focus on the structural, magnetic and electric characterization of MgO and rutile crystals implanted with high fluences of Co and Ni ions, and its evolution and stability upon thermal annealings. Extensive characterization of the magnetic properties of the Co- and Ni-implanted MgO crystals unveiled the dependence on the implantation energy, implanted ions and thermal treatments. Measurements of M(H,T) showed superparamagnetic behaviour allowing to indirectly extract the size distributions of the Ni and Co clusters. XRD spectra of these samples confirm the existence and the mean sizes of such clusters. Correlation was found between the local implanted concentration and the mean cluster size. Vacuum annealings were found to promote growth of the nanoclusters that turn ferromagnetic, whereas the RBS-C lattice recovery is only minor. The effect of annealing under different types of atmosphere is now underway. TiO₂-rutile was also studied with different implanted fluences. Superparamagnetism was found in the as-implanted state, along with a dramatic increase of conductivity, but no magneto-resistive effects were found. The electrical behaviour of the as-implanted samples can be described as a variable range hopping transport, probably resulting from the combination of implantation induced defects and the presence of the magnetic ions.

Vacuum annealings promote modification of the aggregates state but with different results for Co and Ni. Co-implanted rutile turns ferromagnetic while Ni aggregates remain superparamagnetic up to 800 °C. The effect on the electrical behaviour is dramatic with the appearance of a pronounced minimum in the $\rho(T)$ resistivity curve (fig.1).

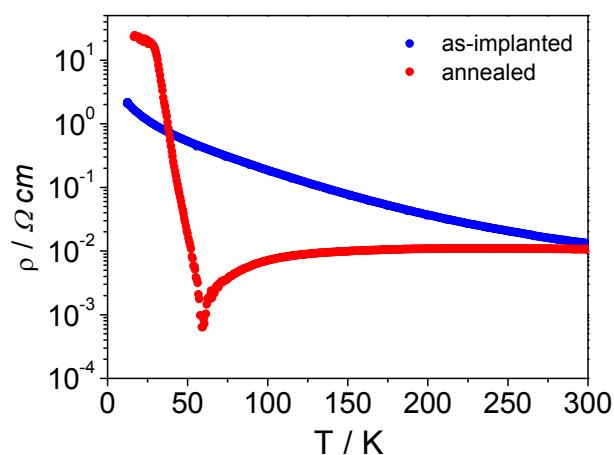


Fig.1. $\rho(T)$ resistivity curves for the as-implanted and vacuum states of Ni-implanted TiO₂-rutile.

Published, accepted or in press work

1. B. Savoini, D. Cáceres, I. Vergara, R. González, R.C. da Silva, E. Alves, Y. Chen, Optical and mechanical properties of MgO crystals implanted with lithium ions, *Journal of Applied Physics*, **95**, 5 (2004) 2371-8.
2. M.M. Cruz, R.C. da Silva, R. González, E. Alves and M. Godinho, Magnetic behaviour of Co and Ni implanted MgO. *Journal of Magnetism and Magn. Materials*, **272-276** (2004) 840-3.
3. J.V. Pinto, R.C. da Silva, E. Alves, Y. Chen, M. Tardío, R. Ramírez, R. González, Electrical conductivity of as-grown and oxidized MgO:Li crystals implanted with Li ions, *Nucl. Instr. and Meth. B*, **218** (2004) 164-69.
4. B. Savoini, D. Cáceres, R. González, J.V. Pinto, R.C. da Silva, E. Alves, Y. Chen, Copper nanocolloids in MgO crystals implanted with Cu ions, *Nucl. Instr. and Meth. B*, **218** (2004) 148-52.
5. J.V. Pinto, R.C. da Silva, E. Alves, M.J. Soares, T. Monteiro, R. González Stability and optical activity of Er implanted MgO, *Nucl. Instr. and Meth. B*, **218** (2004) 128-32.
6. J.V. Pinto, M.M. Cruz, R.C. da Silva and M. Godinho, Magnetic properties of TiO₂ rutile implanted with Ni and Co, *J. Magn. Magn. Mat*, accepted
7. J.V. Pinto, M.M. Cruz and M Godinho, R.C.da Silva, E. Alves, R. González, Magnetic cobalt and nickel nanoaggregates in MgO, submitted PRB.

Encapsulated nanocolloidal dispersions on α -Al₂O₃

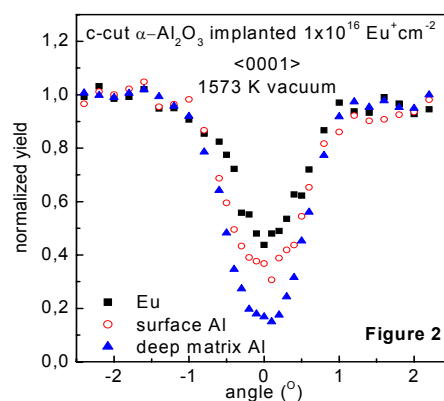
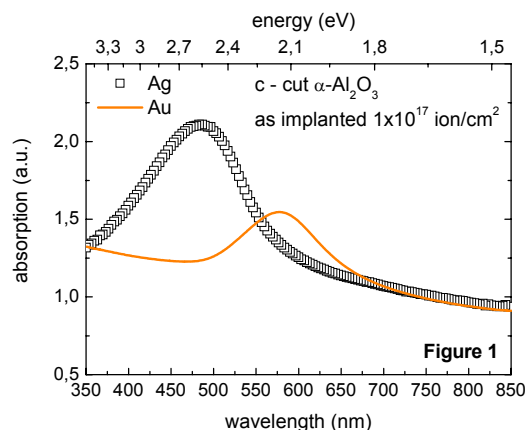
C. Marques, R.C. da Silva, C. McHargue¹, A. Kozanecki², E. Alves

Objectives

Nanoparticles embedded in dielectric matrixes are of great interest, from both the theoretical and application point of views. Most of the physical properties exhibited by these particles are intriguingly different from those of the respective bulk material. Implantation of high fluences and subsequent annealings lead to the formation of colloidal dispersions of precipitates whose optical properties depend on their composition and morphology. On the other hand, low fluences are needed to produce optically active rare-earth dispersions and subsequent annealing tends to redistribute these rare-earths onto lattice regular sites. The implantation fluence, the temperature and type of annealing atmosphere affects both the emission and absorption/reflection bands of these systems in a controllable way, and are being studied.

Results

Optical and structural properties of single crystalline α -Al₂O₃ were changed by the implantation of high fluences of metals (Ag, Cu, Mn, Ni and Au) and low doses of rare-earths (Eu up to now). The optical absorption and reflectance was measured along with some experimental photoluminescence measurements. The system's composition and structure has been analysed through RBS and the morphology of the precipitates inferred through the optical measurements is being compared with x-ray diffraction and transmission electron microscopy. In the case of metals, the main feature of the optical absorption spectra in the visible region is the surface plasmon resonance (SPR) band characteristic of the composition and morphology of the precipitates, as shown in fig. 1 for samples implanted with silver (SPR band peaks at 490 nm) and gold (SPR peaking now at 580 nm). The width and maxima of the SPR band can be varied with the implanted fluence, annealing temperature and atmosphere, allowing tailoring the optical response of the system. In the case of rare-earths, the implantation of low fluencies is preferred in order to produce a lower defect concentration (due to the implantation process) and to avoid the formation of metallic-like aggregates which are optically inactive. Annealing at high temperatures promotes the redistribution of the implanted specie onto regular sites of the matrix, as can be seen in the angular scan on fig. 2. The signal from Eu is similar to that of the matrix elements indicating similar positions (from this axis). For europium ions this means the increase of the characteristic emission in the orange to red region of the visible spectrum.



Published, accepted or in press work

1. C. Marques, E. Alves, R.C da Silva, M.R Silva, A.L. Stepanov, Optical changes induced by high fluence implantation of Au ions on sapphire, *Nucl. Instr. and Meth. B* **218** (2004) 139.
2. E. Alves, C. Marques, L.C. Ononye, C. McHargue, Defect production in nitrogen implanted sapphire, *Nucl. Instr. and Meth. B* **218** (2004) 222.
3. C. McHargue, L.C. Ononye, E. Alves, C. Marques, L.F Allard, The effect of temperature on the structure of iron-implanted sapphire, *Nucl. Instr. and Meth. B* **218** (2004) 227.
4. C. Marques, R.C. da Silva, A. Wemans, M.J.P. Maneira, A. Kozanecki, E. Alves, Site location and optical properties of Eu implanted sapphire, accepted *Nucl. Instr. and Meth. B*.
5. C. Marques, R.C. da Silva, A. Wemans, M.J.P. Maneira, A. Kozanecki, E. Alves, Optical properties tailoring by high fluence implantation of Ag ions on sapphire, accepted *Nucl. Instr. and Meth. B*.

¹ University of Tennessee, USA

² Polish Academy of Sciences, Poland

Magnetic Tunnel Junctions

N. P. Barradas, N. Franco, J.A.V. Gouveia, E. Alves, S. Cardoso¹, P. P. Freitas¹

Objectives

ITN has a long-standing collaboration with the INESC magnetic systems group led by Prof. Paulo de Freitas. The role of ITN is to provide structural characterisation of the highly complex advanced magnetic systems produced at INESC. This is a highly interactive collaboration that has proved to be very successful.

Results

This year the work was concentrated in the compositional and structural characterisation of spin tunnel junctions [1-6]. These are made by two thin magnetic layers separated by a thin insulating one. In tunnel junctions, the tunnelling current across this barrier layer depends on the relative alignment of the magnetisations of the two magnetic layers. Hence such a device can be used either as a reading head (in which the external field - e.g. from a hard disk - leads to a change in the resistance of the system), or as a non-volatile memory (where the external field forces the direction of the magnetisation).

Determination of the composition of the thin to ultra-thin AlN_xO_y layers used in tunnel junctions is not trivial, and is a challenge to analytical techniques in general. On the one hand, we organised a round robin experiments for that purpose, in which 13 laboratories took part [5,6]. On the other hand, we developed an artificial neural network algorithm to analyse the RBS data obtained [6].

Published, accepted or in press work

1. N. P. Barradas, V. Matias, A.D. Sequeira, J. C. Soares, U. Kreissig, J. U. Wang, P.P. Freitas, He-RBS, He-ERDA and heavy ion-ERDA analysis of Si/Ta 70Å/CoFe 35Å/ (Hf 2Å + Al 4Å)oxidation /CoFe 35Å/Ta 30Å systems, *Nucl. Instrum. Methods Phys. Res. B* **219-220** (2004) 742-746.
2. M. Rickart, P.P. Freitas, I.G. Trindade, G. Proudfoot, D. Pearson, M. Davis, N.P. Barradas, E. Alves, M. Salgueiro, N. Muga, J. Ventura, J.B. Sousa, Exchange bias of MnPt/CoFe films prepared by ion beam deposition, submitted to *J. Appl. Phys.*
3. N. Franco, I. V. Yavorovskiy, A. Fonseca, J. A. V. Gouveia, C. Marques, E. Alves, R. A. Ferreira, P.P. Freitas, N. P. Barradas, Rutherford backscattering and x-ray reflectivity analysis of tunnel barriers, *Nucl. Instrum. Methods Phys. Res. B* (accepted).
4. N.P. Barradas, A round robin characterisation of the thickness and composition of thin to ultra-thin $\text{AlN}(\text{O})$ films IAEA TECDOC-1409 (2004) 23-28.
5. N.P. Barradas, N. Added, W.M. Arnoldbik, I. Bogdanović-Radović, W. Bohne, S. Cardoso, C. Danner, N. Dytlewski, P.P. Freitas, M. Jakšić, C. Jeynes, C. Krug, W. N. Lennard, S. Lindner, C. Linsmeier, Z. Medunić, P. Pelicon, R.P. Pezzi, C. Radtke, J. Röhrich, T. Sajavaara, T.D.M. Salgado, F.C. Stedile, M.H. Tabacniks, I. Vickridge, A round robin characterisation of the thickness and composition of thin to ultra-thin AlNO films, *Nucl. Instrum. Methods Phys. Res. B* **227** (2005) 397-419.
6. N.P. Barradas, A. Vieira, V. Matias, G. Öhl, J.C. Soares, S. Cardoso, P.P. Freitas, Development of artificial neural networks for thin Al_xNyO_z films measured by Rutherford backscattering, IAEA TECDOC-1409 (2004) 29-36.

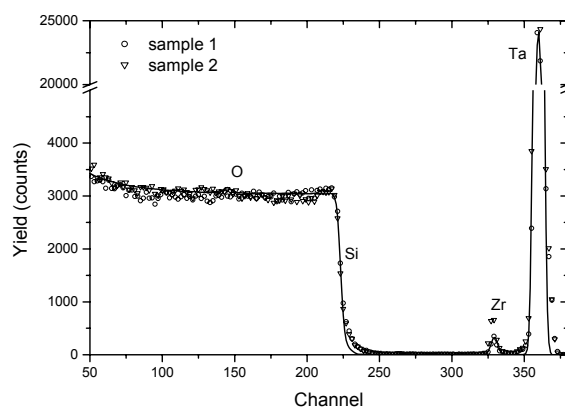


Fig. 1. RBS spectra of samples S1: Si(001)/Zr 5Å/Ta 100Å ; S2: Si(001)/Zr 10Å/Ta 100Å.

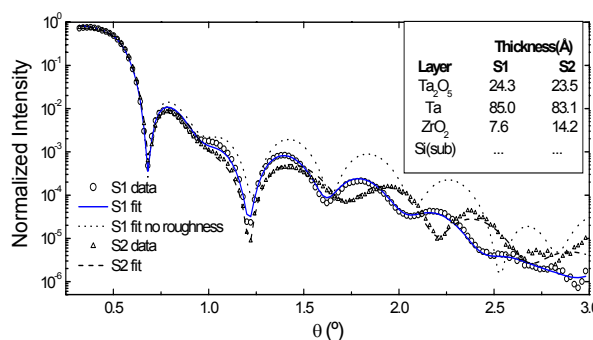


Fig. 2. X-ray reflectivity of samples S1 and S2.

¹ INESC, R.Alves Redol 9-1,1000 Lisboa, Portugal

Study of erbium and silver implanted in silica-titania sol-gel films

A.R. Ramos, C.P. Marques, E. Alves, A.C. Marques¹, R.M. Almeida¹

Objectives

Sol-gel processing is one of the most inexpensive and versatile methods for the fabrication of silica-on-silicon waveguides, including Er³⁺-doped silica-titania planar waveguides. However, the presence of residual OH species in the material limits the fluorescence performance of the Er³⁺ ions. The incorporation of silver metal nanoparticles has been shown to enhance Er³⁺ photoluminescence (PL). The present work tries to address the above-mentioned problems using ion implantation to introduce Er and Ag in silica-titania sol-gel processed films.

Results

Using ion implantation, it was possible to incorporate both Er and Ag in silica-titania films in a controlled and reproducible way. We have implanted silica-titania films, deposited by spin-coating on silica and silicon substrates, with 3×10^{15} at/cm², 180 keV Er⁺ ions and 6×10^{16} at/cm², 140 keV Ag⁺ ions. The energies were chosen so that the profiles of Ag and Er overlapped. Rutherford Backscattering Spectrometry and Elastic Recoil Detection Analysis were used to study the behaviour of Ag, Er and H atoms during the heat treatments used to densify the films. Implantation causes H depletion at the film surface and an increase in H concentration just beneath the implanted Ag and Er profiles. The total H content decreases by 40% to 70% during implantation. During annealing, the H content decreases, with an almost complete H loss after annealing for 35 minutes at 800°C. The Ag profile remains stable up to 600°C. Above 700°C, Ag becomes increasingly mobile. Annealing at 800°C for 35 min results in a nearly constant Ag distribution in the film. The Er profile remains unchanged with the heat treatments, up to the maximum temperature used (800°C). Optical activation of the Er ions was achieved after annealing at 800°C for 95 min.

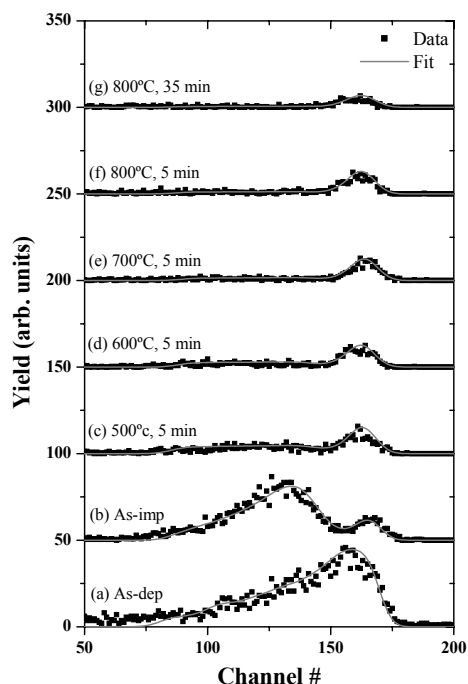


Fig. 1. ERD spectra of Si deposited samples implanted with Ag and Er (24° scattering angle detector, 78° tilt). (a) As deposited; (b) as implanted; (c) 500°C, 5 min anneal; (d) 600°C, 5 min anneal; (e) 700°C, 5 min anneal; (f) 800°C, 5 min anneal; (g) 800°C, 35 min anneal.

Published, accepted or in press work

1. E. Alves, A.R. Ramos, A.C. Marques, R. M. Almeida, Study of silica-titania films doped with Er and Ag by RBS and ERDA, *Nucl. Instr. and Meth.*, **B219-220** (2004) 923.
2. A.C. Marques, R.M. Almeida, E. Alves, A.R. Ramos Compositional profiles in silica-based sol-gel films doped with erbium and silver, *J. of Sol-Gel Science and Technology* **31** (2004) 287.
3. A.R. Ramos, C.P. Marques, E. Alves, A.C. Marques, R.M. Almeida, Stability of erbium and silver implanted silica-titania films” (accepted for publication in *Nucl. Instr. and Meth.*,)

¹Dep. Eng. de Materiais / ICEMS, Instituto Superior Técnico, Av. Rovisco Pais, 1049-001 Lisboa, Portugal

The Characterization of Silicon Carbide Thin Films and Their Use in Colour Sensors

S. Zhang^{1,2}, L. Raniero¹, E. Fortunato¹, X.Liao², Z.Hu², I. Ferreira¹, H. Águas¹, A. R. Ramos, E. Alves, R. Martins¹

Objectives

Due to its adjustable band gap in the visible range of the energy spectrum, hydrogenated amorphous silicon carbide ($a\text{-Si}_{1-x}\text{C}_x\text{:H}$) films are widely used in optoelectronics. In previous works, $a\text{-Si}_{1-x}\text{C}_x\text{:H}$ films with different optical band gaps from 1.83 to 3.64 eV were obtained by adjusting the plasma parameters using plasma enhanced chemical vapour deposition (PECVD). It has been shown that the hydrogen dilution ratio plays a very important role in the deposition conditions. Here, a series of $a\text{-Si}_{1-x}\text{C}_x\text{:H}$ films with different hydrogen dilution ratios were prepared to investigate its influence on the microstructural and photoelectronic properties.

Results

The results show that a higher hydrogen dilution ratio enhances the incorporation of silicon atoms in the amorphous carbon matrix for carbon-rich $a\text{-Si}_{1-x}\text{C}_x\text{:H}$ films.

A one pin structure was prepared using the $a\text{-Si}_{1-x}\text{C}_x\text{:H}$ film as the intrinsic layer. The light spectral response shows that this structure fits the requirement for the top junction of a colour sensor.

Published, accepted or in press work

1. S. Zhang, L. Raniero, E. Fortunato, X.Liao, Z.Hu, I. Ferreira, H. Águas, A.R. Ramos, E. Alves, R. Martins, The characterization of silicon carbide films and their use in colour sensor, Int. Conf. Physics, *Chemistry and Engineering of Solar Cells*, 13-15 May, Badajoz, Spain, J. of Materials Science.

¹Dep. de Ciência dos Materiais, Faculdade de Ciências e Tecnologia, Universidade Nova de Lisboa and CEMOP/UNINOVA, 2829-516 Caparica, Portugal

²State Key Laboratory for Surface Physics, Institute of Semiconductors & Center for Condensed Matter Physics, Chinese Academy of Sciences, Beijing 100083, China

Studies on MgO Solubility in SrTiO₃ Thin Films

O. Okhay¹, A. Wu¹, P. M. Vilarinho¹, I. M. Reaney², A.R. Ramos, E. Alves

Objectives

SrTiO₃ (ST) is an important dielectric material for various electrical applications such as voltage tunable filters, oscillators and phase shifters for microwave circuits. The properties of ST can be dramatically changed by forming solid solutions with cations such as Ba²⁺ or by doping with cations such as Ca²⁺. Theoretical studies predict the appearance of a ferroelectric type anomaly by doping with Mg. However, the incorporation of Mg into the A site of the ST lattice is very limited and consequently no electric anomaly was ever observed. A higher solubility of Mg in the ST lattice is expected for thin films. In this work ST films doped with various Mg concentrations and annealed at different temperatures were grown on Pt/TiO₂/SiO₂/Si substrates by sol-gel. The solid solubility of Mg on ST lattice was studied by TEM and complemented by XRD and RBS analysis.

Results

TEM results revealed homogeneous monophasic

microstructures with small grains for all the compositions annealed at 750°C without any amorphous top layers. For higher annealing temperatures, bigger grains of a second phase rich in Mg were observed and identified with an ilmenite type structure by ED analysis.

RBS indicates that for $x < 0.3$ and for both annealing temperatures Mg is homogeneously distributed all over the film thickness.

XRD analysis corroborates TEM results identifying the Mg rich phase as MgTiO₃.

Published, accepted or in press work

1. O. Okhay, A. Wu, P. M. Vilarinho, I. M. Reaney, A. R. Ramos, E. Alves, Studies on MgO solubility in SrTiO₃ thin films, XXXIX^a Reunião da Soc. Port. Microscopia Electrónica e Biologia Celular, Aveiro, November 2004.

¹Dep. Engenharia Cerâmica e do Vidro, CICECO, Univ. Aveiro, Portugal

²Sheffield University, U.K.

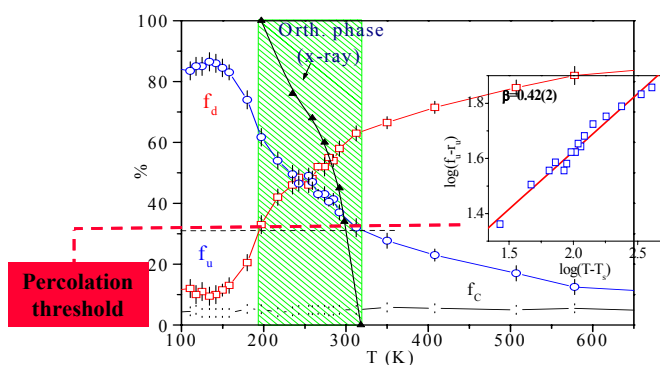
Hyperfine interactions on materials with strong electronic correlations

J.G. Correia, A.M.L. Lopes¹, V. Amaral¹, J.P. Araújo¹, H. Haas, E. Rita, T. M. Mendonça², E. Alves, U. Wahl, M.R. da Silva³, A.C. Marques³, J.C. Soares³ and the ISOLDE collaboration⁴

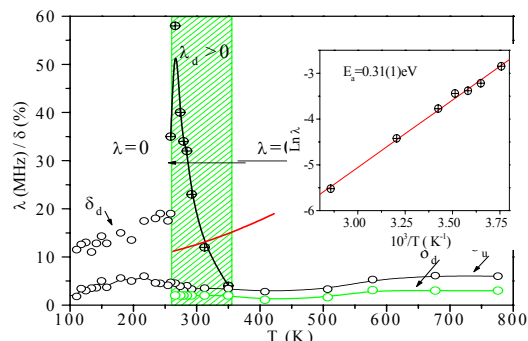
Objectives

We apply hyperfine (PAC) techniques, working with radioactive isotopes, to study local charge and lattice order phenomena into high- T_c superconductors of the form Hg-Ba-Ca-Cu-O ($T_C > 130$ K)" - ref. IS360 CERN- and to materials with giant magnetoresistance, manganites – ref. IS390. For IS360 a new addendum has been approved in 2004 by the CERN-INTC scientific committee to study the ordering of high oxygen concentrations on High- T_C materials. The aim is to disentangle if there is a relationship between collective dopant order and charge ordering. During 2004 samples of Hg1212 and Hg1223 have been synthesized and characterised to me measured during 2005. In what concerns IS390 – Manganites, the studies have shown the existence of slow polaron dynamics within an extended orthorhombic –rhombohedral transition – not detectable by traditional crystallographic techniques – on $\text{LaMnO}_{3,12}$. These results open new perspectives of studies and understanding of the relationship between lattice parameters and electron/spin dynamics on a broader range of doped manganites and other magnetic oxides. This work is performed at the ITN-CFNUL infrastructure at CERN/ISOLDE and is lead by a collaboration of several national institutes.

Results



The blue/red dots are the fractions of undistorted / distorted domains in $\text{LaMnO}_{3,12}$, as a function of temperature. The insert shows the β parameter which value indicates a free percolation of the phase domains on a 3D lattice. X-ray diffraction is not sensitive to the local phase coexistence outside of the percolation thresholds due to the fractal and/or dynamic nature of clusters.



λ is the measured transition frequency PAC parameter for a dynamic interaction, which in the percolative (green) zone reveals to be thermally activated with 0.31eV. The green zone is the observable region of PAC in the intermediate regime. Both below and above this zone there are ultra slow and too fast transitions, respectively, to be quantified.

Published, accepted or in press work

1. J.G. Correia, J.P. Araújo, et. al. Proposal approved by the scientific committee of the ISOLDE-CERN 2004 “Studies of High- T_c Superconductors Doped with Radioactive Isotopes”, CERN-INTC-2004-006, P-86 Add. 2 CERN/ISC 96-30, ISC P86, IS360.
2. A.M.L. Lopes, J.P. Araújo, E. Rita, J.G. Correia, V.S. Amaral, R. Suryanarayanan and the ISOLDE Colaboration, Local Probe Studies on $\text{LaMnO}_3+\delta$ Using the Perturbed Angular Correlation Technique, *J. Magnetism and Magnetic Materials*, **E1671** (2004) 272-276.
3. A.M.L. Lopes, J.P. Araújo, E. Rita, J.G. Correia, V.S. Amaral, Y. Tomioka, Y. Tokura, R. Suryanarayanan and the ISOLDE Colaboration, Perturbed Angular Correlation Study of $\text{Pr}_{1-x}\text{Ca}_x\text{MnO}_3$, *J. of Magnetism and Magnetic Materials*, **E1667** (2004) 272-276
4. J.P. Araújo, A.M.L. Lopes, T. Mendonça, E. Rita, J.G. Correia, V.S. Amaral, and the ISOLDE Colaboration, Electrical Field Gradient studies on $\text{La}_{1-x}\text{Cd}_x\text{MnO}_{3+\delta}$ system. *Hyperfine Interactions*, accepted..

¹ Dep. de Física, Universidade de Aveiro, 3810-193 Aveiro

² IFIMUP, Dep. de Física, Universidade do Porto, Porto

³ CFNUL, Av. Prof. Gama Pinto 2, 1699 Lisboa

⁴ CERN, CH-1211 Geneva 23, Switzerland

Characterisation of Nuclear Fusion Reactor Materials

L.C. Alves, E. Alves, A. Paúl¹, N. Barradas, N. Franco, M.R. da Silva, A. La Barbera², J.B. Hegeman³, F. Druyts⁴

Objectives

Study of erosion/deposition processes in the walls of a Tokamak through the analysis of the graphite tiles exposed to large plasma fluences ($>10^{26} \text{ m}^{-2}$). Evaluation of the impurity contents and distribution in new SiC/SiC_f composites. Phase formation and temperature stability of titanium beryllides.

Results

Nuclear Microprobe, Atomic Force Microscopy (AFM) and Elastic Recoil Detection Analysis (ERDA) techniques were used to characterise the surface morphology and composition of graphite tiles exposed to large plasma fluences in a Tokamak. The difference on elemental surface contents as a function of the tiles position on the Tokamak was established as well as the extent of the modified layer (6-9 μm - fig.1). The ERDA analysis allowed the determination of the T and H deposition profile.

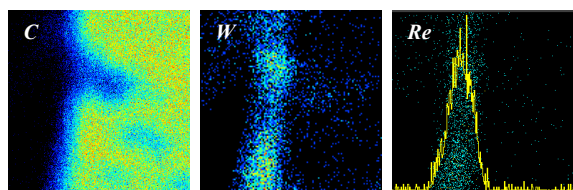


Fig. 1. Elemental distribution on a cross-section of one of the analysed graphite samples. The maps represent an area of $53 \times 53 \mu\text{m}^2$. The Re intensity profile is also shown as well as the C map that is used for defining the sample surface position.

For the SiC composites, not only the high purity of the base materials used for its manufacture was ascertained but also that the detected impurities were due to handling, mainly due to the sample cutting procedure.

Beryllium-titanium intermetallic compounds with a nominal composition of Be-5at%Ti and Be-7at%Ti were analysed by Ion Beam and high-resolution X-ray diffraction techniques. The contaminants observed during a previous analysis of Be pebbles are again revealed. Among them the U that has undesired properties for generating long lived isotopes under neutron bombardment. In the as cast samples, Be₁₀Ti was the major phase formed in the Be-7at%Ti sample while the Be₁₂Ti was the phase observed in the Be-5at%Ti sample.

The Be-5at%Ti alloy reveals intra-grain regions with high concentration of impurities (O, Fe and Ni) and Ti depletion. During thermal treatments up to 800°C for 1 hour, the phase stability was confirmed. Oxidation occurs preferentially at the beryllide grain boundaries in spite of a continuous increase of oxygen that was also found in the beryllide grains (fig. 2).

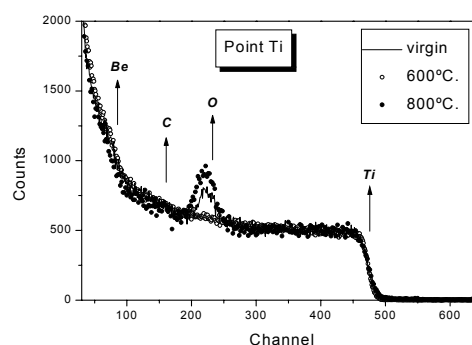


Fig. 2. RBS spectra obtained from a Be₁₂Ti region for the Be-5%Ti alloy before and after annealing.

Published, accepted or in press work

1. E. Alves, L.C. Alves, N. Franco, M.R. da Silva, A. Paúl, J.B. Hegeman, F. Druyts, Characterization and stability studies of titanium beryllides, *Fusion Engineering and Design*, accepted.
2. E. Alves, L. C. Alves, N.P. Barradas, Characterisation of the surface morphology of ASDEX – upgrade Tokamak tiles exposed to large plasma fluences ($>10^{26} \text{ m}^{-2}$), European Fusion Development Agreement, Association Euratom/IST, TASK: TW3- TPP-ERCAR, Final Report (2004).
3. L.C. Alves, A. Paúl, E. Alves, Morphological Characterisation and Impurity Studies of SiC/SiC Composites, European Fusion Development Agreement, Association Euratom/IST, TASK: TW3- TTMA 001 – Deliverable D1, Final Report (2004).

¹ ICMSE, Univ. of Seville-CSIC, Seville, Spain.

² FZK, Forschungszentrum Karlsruhe, Germany.

³ NRG, Petten, The Netherlands.

⁴ SCK-CEN, Belgium.

Ion beam synthesis of inter metallic compounds in light structural metals, aluminium and titanium

L. Prudêncio and R.C. da Silva

Objectives

Ion beams were used to modify the surface region of aluminium and titanium. In particular intermetallic phases can form embedded in these light metals matrices. The so formed surface layers can act as a protection against corrosion and/or improve wear resistance.

Our work concentrated on the direct ion beam synthesis of intermetallic precipitates embedded in the surface region of Al and Ti, and on the study and characterization of its structural properties and stability.

Results

In Aluminium

High purity polycrystalline Al disks were implanted either with Fe, Cr, Ti or Cu, with fluences in the range $1\text{-}5 \times 10^{17}$ /cm², at different substrate temperatures.

Al-Fe system: characterization by RBS, CEMS, GIXRD and SEM lead to the conclusions: *i*) implantation at RT produces the decagonal variant of quasi-crystalline Al₈₆Fe₁₄. *ii*) Above 200 °C the implantations lead to Al₅Fe₂. *iii*) Annealing induces the transformations Al₈₆Fe₁₄ → Al₆Fe → Al₆Fe + Fe(Al) → Al₁₃Fe₄ + Fe(Al) Al₅Fe₂ → Al₅Fe₂ + Fe(Al) → Al₁₃Fe₄ + Fe(Al).

Al-Cr system: characterization by RBS and GIXRD lead to the conclusions: *i*) implantation at RT produces Cr(Al). *ii*) At 400 °C the implantations produce the quasi-crystalline phase Al₈₆Cr₁₄ and above 500 °C lead to Al₁₃Cr₂. *iii*) Annealing induces the transformation Cr(Al) → Al₈₆Cr₁₄ → Al₈₆Cr₁₄ + Al₁₃Cr₂ → Al₁₃Cr₂.

Al-Ti system: characterization by RBS, GIXRD and SEM showed: *i*) implantation at RT leads to formation of AlTi₃ precipitates. *ii*) At 300 °C the implantations produce Ti(Al). *iii*) Above 500 °C the implantations lead to formation of Al₃Ti. *iv*) Annealing induces the transformation AlTi₃ + Ti(Al) → Al₃Ti + Ti(Al).

Al-Cu system: characterization by RBS and GIXRD showed: *i*): implantations at RT leads to formation of Al₄Cu₉ precipitates. *ii*) At 300 °C the implantations produce Al₂Cu. *iii*) Above 500 °C the implantations lead to the solution Cu(Al). *iv*) Annealing induces the transformation Al₄Cu₉ → Al₂Cu → Cu(Al).

In Titanium

Cr implantations were performed in polycrystalline Ti disks, with fluences ranging from 5×10^{16} /cm² to 1×10^{18} /cm² and at different substrate temperatures. Implantations at -180 °C, -110 °C, RT, 200 °C and

300 °C produce the solution Cr(α-Ti), while at 800 °C produce precipitates of the Laves phase α-TiCr₂. When the implantations are carried out at 900 °C a film of Cr(β-Ti) on α-Ti is formed. Annealings induce the transformation Cr(α-Ti) → Cr(β-Ti) + α-Ti.

Long range diffusion of Cr into Ti was found, with two different diffusion regimes occurring at temperatures below and above 800 °C, when annealing is performed directly on RT implanted samples.

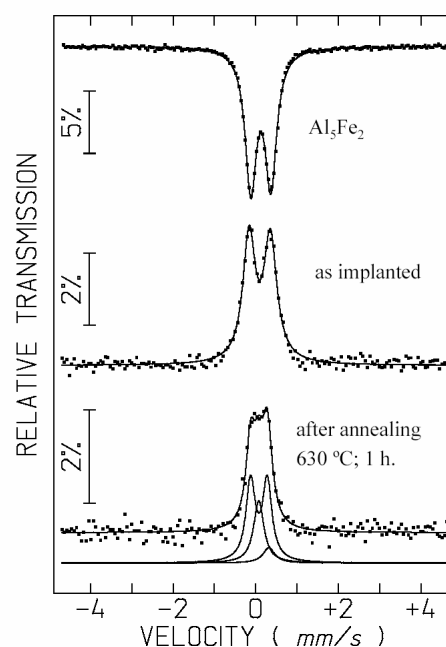


Fig.1. CEMS spectra of implanted samples, as-implanted and after 630 °C annealing, against transmission MS spectrum of a bulk Al₅Fe₂ sample.

Published, accepted or in press work

1. L.M. Prudêncio, L. Paramês, O. Conde and R.C da Silva, Cr ion implantation into Ti – Part I: formation of intermetallic Laves phase, *Surf. & Coatings Tech.*, accepted.
2. L.M. Prudêncio, M. Vilarigues, L.C. Alves and R.C. da Silva, Cr ion implantation into Ti – Part II, Cr diffusivity, *Surf. & Coatings Tech.*, accepted.
3. L.M. Prudêncio, Estudo de Fases Intermetálicas em ligas de Ti e Al formadas por Implantação Iónica, *Ph.D. thesis* in Applied Physics, Univ. Nova de Lisboa, accepted.

Study and Experimental Modelling of Potash Glasses

M. Vilarigues and R.C. da Silva

Objectives

Deterioration of medieval stained glasses of potassium -rich compositions, as the ones found in the XV century Monastery of St. Maria da Vitória, at Batalha, Portugal, is mainly attributed to the very high humidity in the monument, reported higher than 90 %, both indoors and outdoors [1]. A better understanding of the processes leading to deterioration is of fundamental importance to the proper preservation of these glasses.

With this aim in mind, model glasses with SiO-CaO-K₂O ratios similar to those in the composition of Batalha Monastery stained glasses [2], were produced and exposed to immersion essays in distilled water to simulate the high humidity environment.

In particular we expect to obtain information about the ion exchange processes and the kinetics of the reactions involved.

Results

Characterization of corrosion mechanisms in SiO₂-CaO-K₂O based glasses

The work focus on the characterization of corrosion processes of the model potash-glasses in aqueous solutions. Ion beam spectroscopic techniques, Scanning Electron Microscopy and Fourier Transform Infra-Red analysis were used to provide information about the changes in the corroded surface, and combined with evaluation of the changes in the electrolyte solution. In particular hydrogen profiles were obtained by ERD, Elastic Recoil Detection, and the hydrogen uptake correlated with the variation of the pH values of the electrolyte.

Two types of essay have been performed, with and without stirring of the aqueous solution, aiming at simulating separately the effects of water condensation and exposition to rain water.

In any case the experimental data expressed in $Q-t^{1/2}$ coordinates, with Q the amount of material escaped from the glass and t the essay duration, cannot be fitted by a straight line issuing from the origin (Fick's diffusion). Instead the pH evolution in time, Fig.1, can be described by a Boltzmann function. Evolution rates are faster under stirring.

The spectroscopic techniques allowed measuring the K-H exchange revealing a loss of K and uptake of H, along with formation of a silica and carbonate rich layer at the surface. However, the results can only be understood in correlation with the pH evolution if one admits that dissolution of glass has taken place.

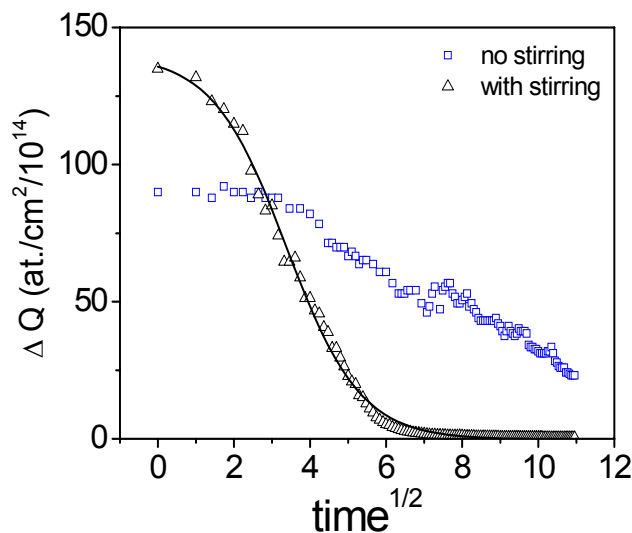


Fig.1. Evolution of concentration of hydronium ions in solution as calculated from the pH of distilled water with glass samples immersed. Longer immersion periods yield similar behaviour.

Published, accepted or in press work

1. M. Vilarigues and R.C. da Silva, Ion beam and Infrared analysis of medieval stained glass, *Applied Physics A*, **79**(2004) 373-378.

High-Resolution X-ray Diffraction Study of $\text{Si}_{1-x}\text{Ge}_x/\text{Si}_{1-x}\text{Ge}_x/\text{Si}$ (001) Heterostructures

N. Franco, N. P. Barradas, E. Alves

Objectives

The introduction of SiGe to standard Si-MOSFET technology allows bandgap engineering with enhanced performance of HMOS transistors. High hole mobility can be realized in n-type modulation doped $\text{Si}_{1-x}\text{Ge}_x/\text{Si}_{1-y}\text{Ge}_y/\text{Si}(001)$ heterostructures, in which a strain-relaxed $\text{Si}_{1-y}\text{Ge}_y/\text{Si}(001)$ buffer with low threading dislocation density has been used as a virtual substrate (VS) for the growth of a $\text{Si}_{1-x}\text{Ge}_x$ channel. To optimise the buffer design and the growth conditions, it is important to know the strain status of the VS and channel. In the present work (224) reciprocal space maps (RSMs) are used to study the thermal stability and strain relaxation mechanisms after pos-growth furnace annealing treatments in N_2 ambient and 650°C .

Results

To study thermal stability and strain relaxation mechanism, ex-situ post-growth furnace thermal treatments were done at various temperature and samples.

2 nm Si
20 nm $\text{Si}_{0.4}\text{Ge}_{0.6}$
16 nm Ge Channel
15 nm $\text{Si}_{0.4}\text{Ge}_{0.6}$
5 nm $\text{Si}_{0.4}\text{Ge}_{0.6}$, $2 \cdot 10^{18} \text{ cm}^{-3} \text{ B}$
20 nm $\text{Si}_{0.4}\text{Ge}_{0.6}$
$\sim 7 \mu\text{m}$ Linear Graded Layer $\text{Si}_{1-x}\text{Ge}_x$, $x \in [0, 0.6]$
n-Si (001) Substrate

Fig. 1. Structure of the SiGe transistor

Six regions are clearly visible in the (224) reciprocal space maps (fig. 2): the intense and narrow Si substrate peak; the intermediate region containing the graded and constant buffer layer; two more distinguish Ge content regions and the 16 nm thick channel peak.

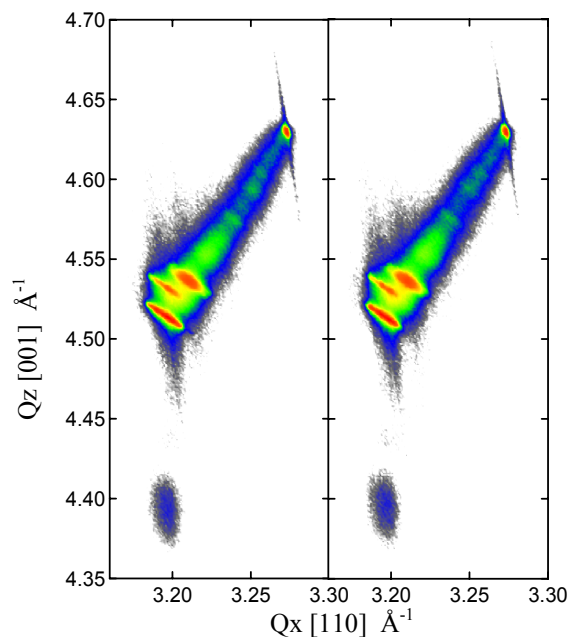


Fig. 2. XRD (224) RSMs of SiGe transistor; as grown on the left and annealed on the right.

The RSMs shows that the graded layer is almost linear and is fully relaxed until a dense region of 48% of Ge, after that there is another two dense regions of 53% and 60%, where the 53-54% region is fully strained.

Due to peaks width, it is not possible to distinguish the layers that have close Ge content. The Channel has a Ge concentration of 97 % and is fully strained, and it was estimated in 20 nm.

A tilt in graded layer increasing from bottom to the top is also observed. Comparing both RSMs, they are almost undistinguished. Only a slight difference between the peaks shape, the annealed peaks are sharper. This means a possible crystalline quality improvement and/or a lower roughness between layers.

Published, accepted or in press work

1. A. Fonseca, N. Franco, E. Alves, N. P. Barradas, J. Leitão, N. A. Sobolev, D. Badonneau, High resolution backscattering studies of nanostructured magnetic and semiconducting materials, accepted for publication.

Formation of Ge Nanoparticles by Oxidation of Thin $\text{Si}_{1-x}\text{Ge}_x$ Layers

A. Kling, J.C. Soares¹, C. Prieto², J. Jimenez², A. Rodríguez³, J. Sangrador³, T. Rodríguez³

Objectives

Nanoparticles of Ge embedded in a dielectric matrix formed appear as very promising systems for electronic and photonic applications. The formation of Ge nanocrystals with uniform size, less than 5 nm, embedded in a dielectric medium is an essential process for the fabrication of electronic and photonics devices which can be easily integrated with the Si-based electronic circuits. One of the methods to form them is by dry thermal oxidation of SiGe alloys. Detailed characterization of the oxidation process in polycrystalline SiGe layers from the non-oxidized state to the full oxidation of the layer is highly important in order to understand the processes involved.

Results

We have characterized the dry oxidation process at 850°C of a 50 nm SiGe layer deposited by LPCVD on a 6000 nm SiO_2 layer using RBS, FTIR and Raman spectroscopy [1]. The RBS studies revealed that in a first step Si-Si bonds are oxidized growing SiO_2 , forcing Ge to segregates from the SiO_2 . As soon as all Si is oxidized GeO_2 is growing gradually. Fig. 1 shows the layer thickness of SiO_2 and GeO_2 in dependence of the oxidation time as determined by RBS. The growth rates for SiO_2 and GeO_2 in the linear regions are 0.25 and 0.35 nm/min, respectively.

On the other hand, for the reliable determination of the GeO_2 thickness information on the amount of Ge-O bonding had to be obtained from FTIR spectra.

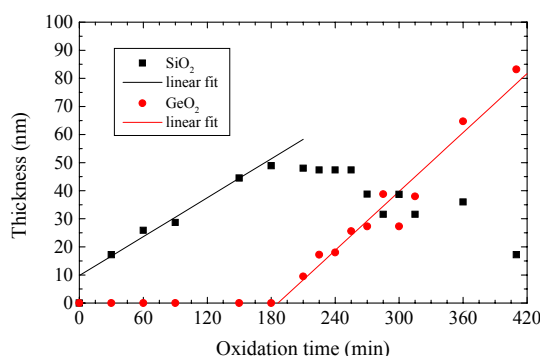


Fig. 1. SiO_2 and GeO_2 layer thickness as a function of the oxidation time.

Figure 2 demonstrates the variations in the absorption bands induced by the changes of the bonding due to oxidation processes. The oxidation of the Ge layer seems to start by the formation of Si-O-Ge bonds. Later on Ge-O-Ge bonds, corresponding to GeO_2 , appear. For longer oxidation times, most of the Ge is found to be bonded as Ge-O-Ge.

In addition, Raman spectroscopy yielded detailed information about the oxidation processes for different bonds (Si-Si, Si-Ge, Ge-Ge).

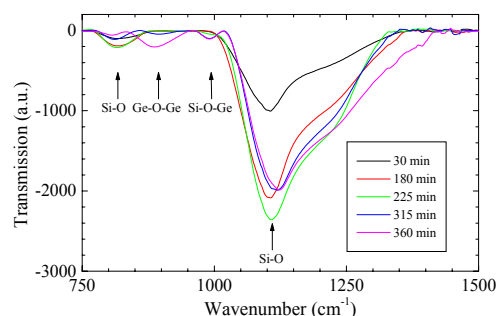


Fig. 2. Variations in the transmission due to changes in the number of bonds give additional information on the evolution of the oxidation processes.

Published, accepted or in press work

1. A. Kling, J.C. Soares, C. Prieto, J. Jimenez, A. Rodríguez, J. Sangrador, T. Rodríguez, Ion Beam Analysis of the Dry Thermal Oxidation of Thin Polycrystalline SiGe Films, *Nucl. Instr. and Meth. B*, accepted for publication.

¹Centro de Física Nuclear da Universidade de Lisboa.

²Dep. Física de la Materia Condensada, E.T.S.I. Industriales, Universidad de Valladolid, Spain

³Dep. Tecnología Electrónica, E.T.S.I. de Telecomunicación, Universidad Politécnica de Madrid, Spain.

Composition studies of Ti-Al-Si-N nanocomposite and Oxynitride Coatings

E. Alves, A. R. Ramos, N. Barradas, F. Vaz¹, S. Carvalho¹, L. Rebouta¹

Objectives

The so-called nanocomposite films, consisting of nanocrystalline transition metal nitrides, MeN, and amorphous Si₃N₄ composites, which have unique mechanical, chemical and tribological properties, have been one of the most promising superhard materials. A wide variety of studies within this nanocomposite system have been performed, in particular on nc-TiN/a-Si₃N₄.

The purpose of this study is to present a comparative analysis of the structure of samples prepared with different low temperature deposition parameters. Coatings using different plasma densities and ion bombardment conditions were prepared, creating conditions to obtain Ti-Al-Si-N films with different properties and structural arrangements.

Results

These results show that different deposition conditions can lead to a maximum hardness values with different structural arrangements. In those arrangements the Si content plays a different role, contributing for a solid solution hardening, a formation of a superhard nanocomposite of the type nc-MeN/a-Si₃N₄ or to a multiphase system where the MeN and Si₃N₄ phases coexist with the solid solution, (Ti,Al,Si)N, which explains how is possible to get maximum peak hardness for different Si content values.

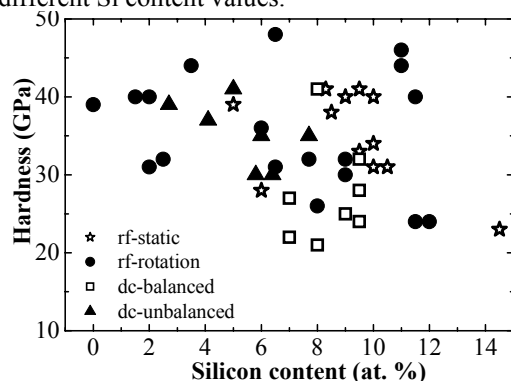


Fig. 1. Dependence of the hardness of Ti-Si-Al-N samples as a function of silicon content.

In order to verify if the oxygen impurities are limiting the achievable hardness, the oxygen contents of seven samples was characterized by ERDA. The results, although scarce, are not contradictory with our conclusions. Favourable conditions for the solid solution formation are some thermodynamic and kinetic constraints (nitrogen activity and energy delivered to the substrate) and Si contents up to 10 at. % in Ti-Al-Si-N films. The relatively low Si content increases the probability of Si atoms as next-nearest neighbors to the Ti

atoms in the TiN arrangement. Increasing the Si content, the Si atoms as next-nearest neighbors to the Si atoms increases, decreasing the proportion of six-fold silicon.

Published, accepted or in press work

1. E. Alves, A. Ramos, N. Barradas, F. Vaz, P. Cerqueira, L. Rebouta, U. Kreissing, Ion beam studies of TiN_xO_y thin films deposited by reactive magnetron sputtering, *Surf. Coat. Technol.* **180-181** (2004) 372-376.
2. S. Carvalho, L. Rebouta, E. Ribeiro, F. Vaz, M.F. Denanot, J. Pacaud, J.P. Rivière, F. Paumier, R.J. Gaboriaud, E. Alves, Microstructure of superhard (Ti,Si,Al)N nanocomposite coating, *Surf. Coat. Technol.* **177-178** (2004) 369-375.
3. L.A. Rocha, E. Ariza, J. Ferreira, F. Vaz, E. Ribeiro, L. Rebouta, E. Alves, A.R. Ramos, Ph. Goudeau, J. P. Rivière, Structural and corrosion behaviour of stoichiometric and substoichiometric TiN thin films, *Surf. Coat. Technol.* **180-181** (2004) 158-163.
4. F. Vaz, P. Cerqueira, L. Rebouta, S.M.S. Nascimento, E. Alves, Ph. Goudeau, J.P. Rivière, K. Pischow, J. De Rijk, Structural, optical and mechanical properties of coloured TiN_xO_y thin films, *Thin Solid Films* **447-448** (2004) 449-454.
5. E. Ribeiro, L. Rebouta, S. Carvalho, F. Vaz, G.G. Fuentes, R. Rodriguez, M. Zazpe, E. Alves, Ph. Goudeau, J.P. Rivière, Characterization of hard DC-sputtered Si-based TiN coating, *Surf. Coat. Technol.* **188-189** (2004) 351-357.
6. F. Vaz, P. Carvalho, L. Cunha, L. Rebouta, C. Moura, E. Alves, A.R. Ramos, A. Cavaleiro, Ph. Goudeau, J.P. Rivière, Property change in ZrN_xO_y thin films: effect of the oxygen and bias voltage, *Thin Solid Films* **469-470** (2004) 11-17.
7. E. Ariza, L.A. Rocha, F. Vaz, L. Cunha, S.C. Ferreira, P. Carvalho, L. Rebouta, E. Alves, Ph. GOUDEAU, J.P. RIVIÈRE, Corrosion resistance of ZrN_xO_y thin films obtained by rf reactive magnetron sputtering, *Thin Solid Films* **469-470** (2004) 274-281.
8. L.A. Rocha, E. Ariza, J. Ferreira, F. Vaz, E. Ribeiro, L. Rebouta, E. Alves, A.R. Ramos, Ph. Goudeau, J.P. Rivière, Structural and Corrosion Behaviour of Stoichiometric and Substoichiometric TiN Thin Films, *Surf. Coat. Technol.* **180-181** (2004) 158.

¹Universidade do Minho, Dep. Física, Azurém, 4800-058 Guimarães, Portugal.

Advanced data analysis for IBA

N. P. Barradas, C. Pascual-Izarra, H. F. R. Pinho, N. R. Nené, A. Vieira¹

Objectives

Ion Beam Analysis (IBA) is a cluster of techniques dedicated to the analysis of materials. Data analysis is normally done in an interactive way, requiring a dedicated expert. Our goal is to automate IBA data analysis.

Results

We developed a new and more efficient artificial neural network (ANN) algorithm to analyse extremely complex data and multiple spectra [1-3]. This closes the line of research in ANNs applied to IBA.

We have previously developed a code, the IBA DataFurnace, that uses the simulated annealing algorithm to automatically analyse IBA data. We recently developed an algorithm to include different models of roughness in RBS data analysis in a fast way. We now investigated the limits of validity and application of the models and methods, and applied them to specific cases [4-6].

We developed a new algorithm to calculate double scattering in RBS, and integrated it in the DataFurnace [7,8].

We used Bayesian inference to determine the stopping power of 4He in different materials [9,10].

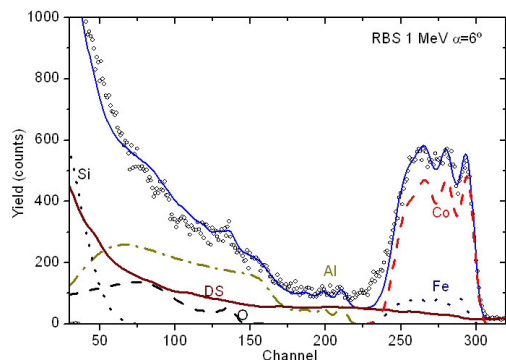


Fig. 1. RBS spectrum of sample Si(100)/Al₂O₃ 500nm/(CoFeB 2 nm/Al₂O₃ 0.9 nm)₄/Ta 2nm collected at 1 MeV and $\alpha=6^\circ$. The Ta signal is not shown. The calculated partial spectra of given elements are shown. The double scattering+pileup contribution is identified as DS.

Published, accepted or in press work

1. N. P. Barradas, R. P. Patrício, H. Pinho, A. Vieira, A general artificial neural network for analysis of RBS data of any element with Z between 18 and 83 implanted into any lighter one- or two-element target, *Nucl. Instrum. Methods Phys. Res. B* **219-220** (2004) 105-109.

2. N.P. Barradas, A. Vieira, V. Matias, G. Öhl, J.C. Soares, S. Cardoso, P.P. Freitas, Development of artificial neural networks for thin Al_xNyO_z films measured by Rutherford backscattering, IAEA TECDOC-1409 (2004) 29-36.
3. H. F. R. Pinho, A. Vieira, N. R. Nené, N.P. Barradas, Artificial neural network analysis of multiple IBA spectra, *Nucl. Instrum. Meth. Phys. Res. B*, in press.
4. N. P. Barradas, E Alves, S. Pereira, V. V. Shvartsman, A. L. Kholkin, E. Pereira, K. P. O'Donnell, C. Liu, C. J. Deatcher I. M. Watson, M. Mayer, Roughness in GaN/InGaN films and multilayers determined with Rutherford backscattering, *Nucl. Instrum. Methods Phys. Res. B* **217** (2004) 479-497.
5. N. P. Barradas, E. Alves, D. Babonneau, Characterization of FePt nanoparticles in FePt/C multilayers, *Nucl. Instrum. Methods Phys. Res. B* **219-220** (2004) 919-922.
6. C. J. Tavares, L. Rebouta, J. P. Rivière, T. Girardeau, P. Goudeau, E. Alves, N. P. Barradas, Atomic environment and interfacial structural order of TiAlN/Mo multilayers, *Surf. Coatings Technology* **187** (2004) 393-398.
7. N.P. Barradas, Double scattering in grazing angle Rutherford backscattering spectra, *Nucl. Instrum. Methods Phys. Res. B* **225** (2004) 318-330.
8. N. P. Barradas, C. Pascual-Izarra, Double scattering in RBS analysis of PtSi thin films on Si, *Nucl. Instrum. Methods Phys. Res. B*, in press.
9. C. Pascual-Izarra, M. Bianconi, N. P. Barradas, A. Climent-Font, G. Garcia, J. Gonzalo, C. N. Afonso, Continuous stopping power curves of Al₂O₃ for 0.2-0.5 MeV He ions, *Nucl. Instrum. Methods Phys. Res. B* **219-220** (2004) 268-272.
10. N.P. Barradas, C. Pascual-Izarra, A. Climent-Font, M. Bianconi, Determination of the stopping power of 4He in thin oxynitride films, IAEA TECDOC-1409 (2004) 37-44.

¹ Instituto Superior de Engenharia do Porto, R António Bernardino de Almeida 431, 4200 Porto.

